CHARA TECHNICAL REPORT

NO. 25 28 DECEMBER 1995

Observing AGNs with an Optical Interferometer

BRIAN MASON & THEO TEN BRUMMELAAR

ABSTRACT: The advent of long-baseline optical interferometry opens up new avenues of analysis in the study of AGNs. The nature of the problem is discussed along with its potential application with the CHARA Array and with a future space-based interferometer.

1. INTRODUCTION

With the burgeoning technology of long-baseline optical interferometry, it will soon be possible to investigate parameters in a regime which is thus far directly unexplored at optical wavelengths: the physical dimensions of the cores of active galactic nuclei (AGNs). The small-scale structure and surface flux characteristics of this class of objects are largely unknown, but with known or estimated parameters it is possible to determine which objects can be studied and what may be determined.

Over the past several years AGN theory has undergone a transformation from a variety of morphological types to the now widely accepted unified model (Antonucci 1993). In this current construct, AGNs can be divided into two basic groupings: radio quiet and radio loud. Other subdivisions of AGN types are a product of the beaming angle of the jet and the distance (age). As a result of this, gross structure of all AGNs can be estimated to zeroth order by adequately investigating one subclass. Consequently, the closest AGNs, Seyfert galaxies, will have the largest projected core size and will allow the first direct measurement of the spatial dimensions of this class of object.

AGNs are believed to arise from a supermassive black hole surrounded by a hot accretion disk a few light days across. Beyond this disk is the high density broad-line region (BLR) with permitted transitions and line widths in the neighborhood of a few thousand $\mathrm{km\,s^{-1}}$, and the lower density narrow-line region with both permitted and forbidden transitions and line widths an order of magnitude smaller. Reverberation mapping, a technique measuring the emission-line response of the BLR of Seyferts (Peterson 1993), has yielded sizes in the neighborhood of 10 light days. While it is not certain if this baseline value is representative of this class, Netzer's (1991) model with sizes of from 3 to 60 light days produces results which are consistent with reverberation mapping.

Observing the BLR of these objects with long-baseline optical interferometry offers the opportunity to characterize AGN cores in the following ways:

[1]Center for High Angular Resolution Astronomy, Georgia State University, Atlanta GA 30303-3083
Tel: (404) 651-2932, FAX: (404) 651-1389, Anonymous ftp: chara.gsu.edu, WWW: http://www.chara.gsu.edu

1. Set an upper limit for the angular size of these BLRs.
2. Examine the gross morphology of these objects.
3. Determine whether any ellipticity is co-aligned with the jets.
4. Observe the variation in size contemporaneously with measures of photometric variability.
5. In the case of the nearest Seyferts, see which models of surface flux distribution are consistent with measured visibility profiles.

Another and perhaps more exciting possibility is the analysis of BLR 'cloudlets'. It has been widely conjectured that the BLR is not a single object but consists of many small clouds which orbit the central engine. If the baselines are large enough and these objects have sufficiently long lifetimes, it may be possible to calculate Keplerian orbits for them, and thus determine the mass of the supermassive black hole and its accretion disk.

2. LIMITS ON DIAMETER MEASUREMENTS

The first, and still most common, method of measuring the angular extent of an astrophysical object with an interferometer is to use a uniform disk model for the object. The measured correlation (visibility squared) for such an object is given by (Davis 1981)

$$C = V^2 = \left| \frac{2J_1(\delta)}{\delta} \right|^2 \tag{1}$$

where

$$\delta = \frac{\pi \theta B}{\lambda}, \tag{2}$$

and θ is the angular extent of the object, B is the baseline and λ is the wavelength of the observation. Figure 1 presents a plot of Equation 1 with the first and second minimums and the second peak shown.

By observing the object at several baseline orientations, it is possible to measure the equivalent width in various directions using Equation 1. The simplest method of doing this, indeed the method used by Michelson himself (Michelson & Pease 1921), is searching for the first correlation null at $\delta = 1.22\pi = 3.833$ and solving for θ using Equation 2.

Of course, it is extremely unlikely that the object will in reality be as 'hard-edged' as this model predicts. If the object intensity fades as one moves to the outer edges (for example 'limb darkening' in stars), the correlation curve shown in Figure 1 changes in two important ways: the first correlation null occurs at lower values of δ, and the shape of the second peak changes. In order to measure this effect, one must have baselines out to the second peak, that is at least to $\delta = 1.64\pi = 5.152$. If, on the other hand, one continues to use the uniform disk model, the size of the object will be over-estimated, with the over-estimate being greater for objects less like a uniform disk. In this way a single baseline could at least be used to set an upper limit to the size of an object. More baselines will be required to get more information about the shape and size of the object.

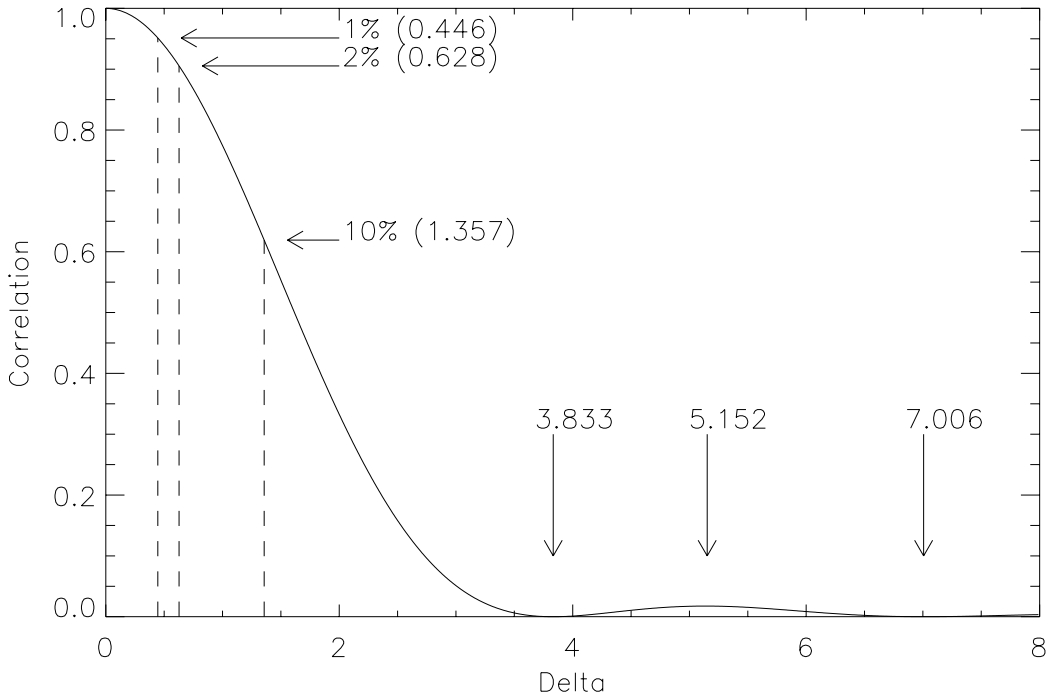

FIGURE 1. Response of an interferometer to a uniform disk object. The horizontal axis is in units of δ defined in Equation 2 and the vertical axis is the visibility squared. The specific points marked on the plot are discussed in the text.

Rather than locating the first null, one need only measure the correlation at a single baseline and wavelength to measure the equivalent width of an object and then use Equations 1 and 2 to solve for θ. The precision of this method will depend strongly on the precision of the correlation measurement. If the percentage error in the correlation measurement is

$$P_C = 100 \times \frac{\Delta C}{C} \tag{3}$$

where ΔC is the absolute error in the correlation measurement and the percentage error required in the angular size measurement is

$$P_\delta = 100 \times \frac{\Delta \delta}{\delta}, \tag{4}$$

one can say that we can move down in values of δ until

$$\frac{dC(\delta)}{d\delta} = -\frac{\Delta C}{\Delta \delta} = -\frac{P_C}{P_\delta} \times \frac{C(\delta)}{\delta}. \tag{5}$$

Using standard recurrence relations for Bessel functions it can be shown that this is true when

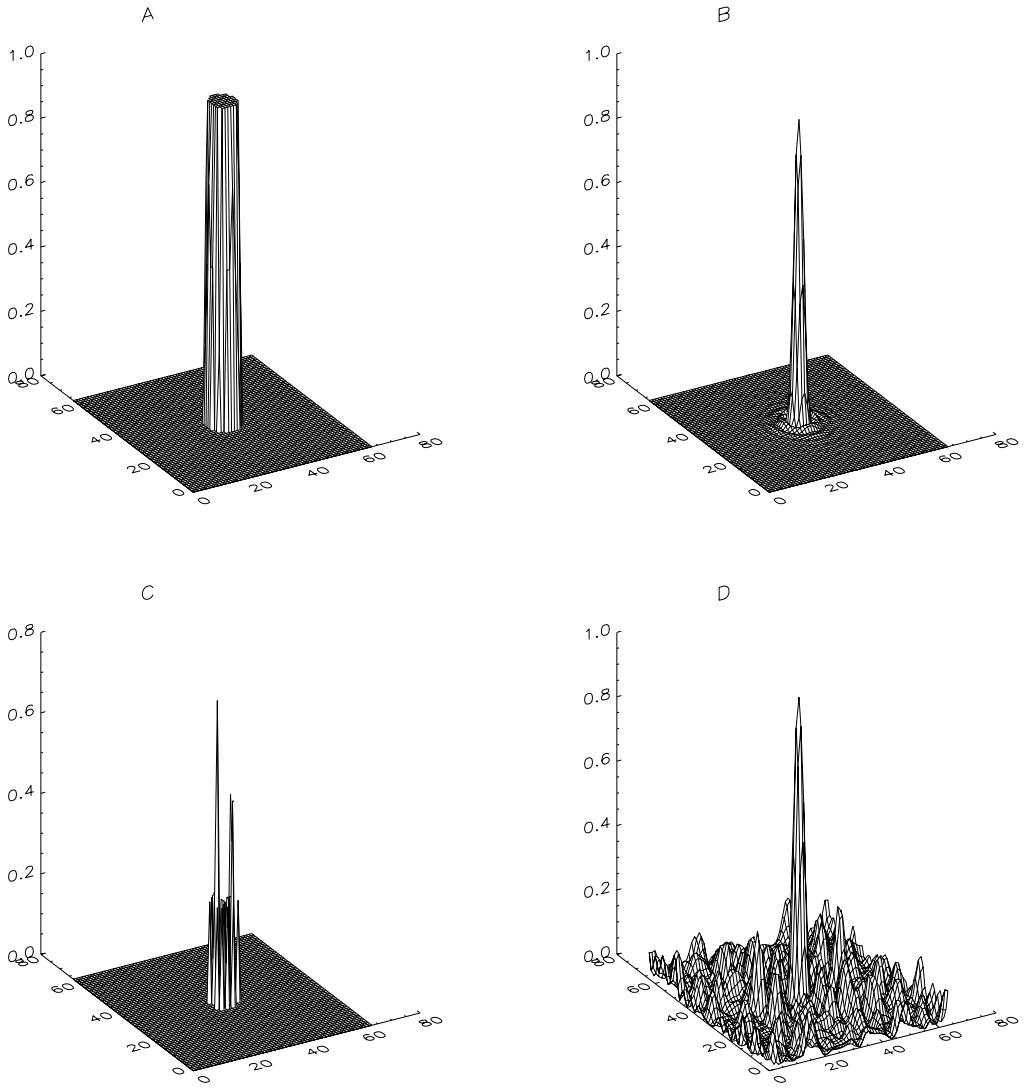

FIGURE 2. Response of an interferometer to a uniform disk object and a series of delta functions. Part A shows a uniform disk, with its UV plane representation is shown in part B. Parts C and D show the same image area filled with randomly generated delta functions, together with their UV plane representation.

$$J_1(\delta)\left[3 - \frac{P_C}{P_\delta}\right] - \delta J_0(\delta) = 0. \tag{6}$$

This has been solved for $P_\delta = 10\%$ and $P_C = 10\%$, 2% and 1% and have been indicated in Figure 1. Table 1 shows the resulting resolution limits of an interferometer based on this equation for the maximum baseline size for the CHARA Array and a 1000 m baseline interferometer observing in Hα and Hβ.

TABLE 1. Resolution limits of uniform disk model in micro-arcseconds. These limits have been calculated for a 354 m and a 1000 m baseline observing in the Hα and Hβ wavelengths. The resolution limits for 'limb darkening', the first correlation null and several values of the precision of correlation measurement are shown, assuming a required precision of 10% on the diameter measurement.

		Baseline = 354 m		Baseline = 1000 m	
	δ	$\lambda = 656.3$ nm	$\lambda = 486.1$ nm	$\lambda = 656.3$ nm	$\lambda = 486.1$ nm
Limb Darkening	5.152	630	470	220	170
First Null	3.833	470	350	170	130
10%	1.357	170	130	59	44
2%	0.628	77	57	28	20
1%	0.446	55	41	20	15

If the BLR is not a continuous object but consists of a large number of small 'clouds' orbiting around the central super-massive object, each of these cloudlets will be too small to resolve without extremely large baselines. They will, however, appear as a series of delta functions assembled inside the area of the BLR. Figure 2 contains an example of the UV plane for such an object. The top line shows a 'hard-edged' circular object on the left and its UV plane representation on the right. The lower two plots are of a random series of delta functions inside the same area as the disk on the left and the UV plane representation on the right. Clearly, if baselines large enough to investigate the outer regions of the UV plane are not available, the delta functions will not be distinguishable from a uniform disk. If these larger baselines are available, it will be possible to show, one way or the other, if the object is continuous or composed of many smaller objects, if not actually image the object.

3. REQUIRED INTEGRATION TIMES AND MAGNITUDE LIMITS

The number of parameters required to calculate the integration time needed to achieve a given signal to noise ratio (SNR) is large, and it is correspondingly difficult to estimate limiting magnitudes. Thus one must choose 'reasonable' values and remember that the resulting limits are only as good as these choices.

The SNR of a correlation measurement depends on the apparent visibility, the average number of photons per sample, the detector noise, and the method of measurement. The modified Tango & Twiss measurement scheme has a SNR given by (ten Brummelaar 1995)

$$\mathrm{SNR}(V^2) = \frac{\sqrt{M}N^2V^2}{4\sqrt{\frac{1}{32}N^4V^4 + \frac{1}{2}N^3V^2 + \frac{1}{2}N^2 + \sigma^2(N^2V^2 + 2N + \frac{1}{2}) + 2\sigma^4}}, \tag{7}$$

where V is the apparent visibility, including atmospheric and optical aberrations, M is the number of samples, N is the expected number of detected photons in a single sample and σ is the standard deviation of the detector noise in a single sample.

We begin by choosing values for the sample time and aperture size. The CHARA Array is to be built on Mount Wilson which has a well documented history of excellent seeing conditions. We therefore set the values of $r_0 = 20\,\mathrm{cm}$ and $\tau_0 = 10\,\mathrm{ms}$. According to the work done by Buscher (1988), the optimum aperture size is approximately $2.5\,r_0$ and the optimum sample time is $1.6\,\tau_0$. We therefore choose an aperture size of 0.5 m and a sample time of 16 ms. We still need to be taken into account the optical throughput of the Array and the detector quantum efficiency in order to move from a stellar magnitude, aperture size, and sample time to an expected photon count rate. The optical throughput to the fringe tracking system (the system best suited to simple correlation measurements) has been estimated to be approximately 16% (ten Brummelaar 1993). The detector quantum efficiency will be set to 40% for a noiseless APD detector and 80% for a CCD with a noise level of 3 electrons.

The atmospheric effects on the visibility are given in Tango & Twiss (1980) for the case of spatial effects and Buscher (1988) for the case of temporal effects. The optical system characteristics must either be measured directly, or estimated for the CHARA Array. Based on the error budget set out for the Array (Ridgway 1994), a Strehl ratio of 0.95 is found for the total optical system at a wavelength of 0.5 microns and an aperture size of 50 cm. This can be used as a coherence transfer factor (ten Brummelaar et al. 1995). The apparent visibility is the 'real' visibility as given by Equation 1 multiplied by the spatial, temporal and optical transfer factors.

It remains to choose an optical bandwidth for the measurement. According to Peterson (1993) the width of the Hα and Hβ lines in the BLR is 1000-10000 $\mathrm{km\,s^{-1}}$. Using the value of 5000 $\mathrm{km\,s^{-1}}$ this corresponds to an optical bandwidth of approximately 10 nm. Figure 3 shows a plot of the required integration time to achieve the accuracies of 10%, 2% and 1% discussed in the previous section for a range of magnitudes. One more parameter must be chosen in order to set limits, the maximum allowable integration time. A horizontal line has been placed on this plot at the two hour level, since after this time the baseline will certainly have changed. However, data from several nights' observations could be added together to achieve longer integration times. Thus, assuming one either has a reference object on which to actively track fringes, or can passively track, it should be possible to measure as faint as 13^{th} magnitude, perhaps fainter. In the case of a space-based platform all of the parameters above change, but due to the possibility of longer integrations times and the absence of atmospheric aberrations it should have a fainter limit than any ground based device.

4. AGN MEASUREMENT WITH THE CHARA ARRAY

In order to be sure that the correct BLR is being measured and not some clumping of dust along the line of sight, a wavelength where the BLR should be very bright is selected. Hα is well suited to this task and will produce enough flux so that the BLR should be resolved. Of practical consideration is establishing a reference on which the fringe tracker will be able to track. The interior structure of these bodies is poorly known and will remain uncertain until observations are made. However, it is not unlikely that the accretion disk may provide a bright enough point source for active fringe tracking. If not, passive tracking methods

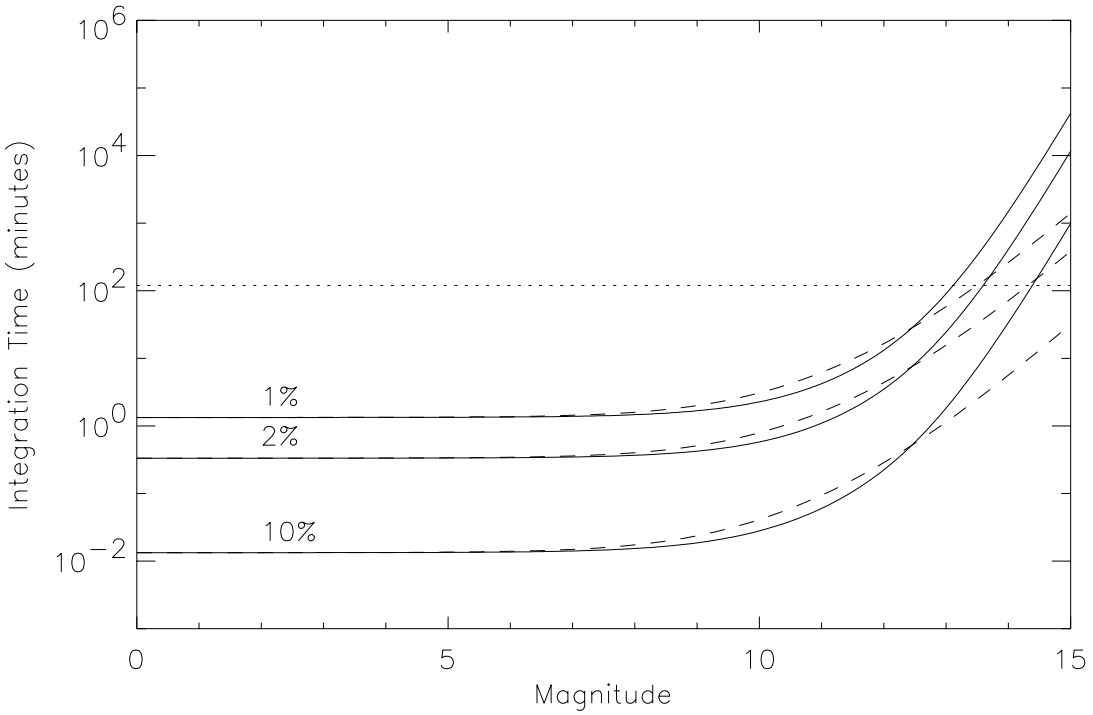

FIGURE 3. Integration time required to achieve the 10%, 2% and 1% precision levels setout in section 2. The solid lines are for a CCD while the dashed lines are for an APD. The dotted horizontal line shows the two hour integration point. The assumptions used to generate this plot are set out in the text.

could be employed.

A list of bright, nearby Seyferts is provided by Weedman (1977). If we assume a physical size of 10 light days and set $H_0 = 75\,\mathrm{km\,s^{-1}\,Mpc^{-1}}$, then the performance of the CHARA Array is as described in Table 2. Also provided in Table 2 are the same performance parameters if the BLR is bright enough in Hβ. This list covers only the portion of the sky accessible with the CHARA Array.

As seen in Table 2, the CHARA Array will be able to make a 'hard-edged' approximation to the size of the BLR of Seyferts. While it is not possible to characterize the BLR structure as described in Section 2, it is possible to obtain a limit as to the physical size of the BLR. Table 3 shows a list of the specific AGNs which should be observable with the CHARA Array. Here the magnitudes in the given bands have been calculated assuming that half of the available flux is within the Hα and Hβ lines and that these lines have the classical ratio of 2.87:1. Almost all of these objects fall within the 13th magnitude limit set out in Section 3 in Hα, and during times of excellent seeing they should also be observable in Hβ. Seyfert type 1 galaxies will be the easiest objects in which to see the BLR, and, while Seyfert 2 galaxies may not clearly exhibit BLR phenomena, they should also be investigated.

TABLE 2. Number of BLRs resolvable with the CHARA Array in both Hα and Hβ given the parameters from Table 1, a physical size of 10 light days and $H_0 = 75\,km\,s^{-1}\,Mpc^{-1}$. The resolution limits for 'limb darkening', the first correlation null and several values of the precision of correlation measurement are shown, assuming a required precision of 10% on the diameter measurement.

	No. of Objects Hα $\lambda = 656.3$ nm	No. of Objects Hβ $\lambda = 486.1$ nm
Limb Darkening	0	0
First Null	0	0
10%	1	2
2%	5	5
1%	5	9

TABLE 3. Objects observable by the CHARA Array.

Object	Seyfert Type	V Mag	Dec	Hα Mag	Hα Best Resolution	Hβ Mag	Hβ Best Resolution
NGC 1068	2	8.91	−00	9.99	5%	11.13	5%
NGC 3227	2	13.52	+20	14.60	5%	15.74	5%
NGC 3516	1	12.30	+73	13.40	—	14.50	1%
NGC 4051	1	11.50	+45	12.60	10%	13.70	10%
NGC 4151	1	11.20	+39	12.30	5%	13.40	10%
Mkn 270	2	14.30	+68	15.40	—	16.50	1%
NGC 6764	2	13.20	+51	14.30	—	15.40	1%
NGC 6814	1	12.00	−10	13.00	5%	14.00	5%

5. SPACE-BASED INTERFEROMETERY OF AGNS

The situation is much more optimistic with a space-based interferometer. The list of accessible objects for making a 'hard-edged' approximation is much larger, and it may be possible to model the morphology of the BLR. Table 4 provides the same data for a space-based interferometer that Table 2 provided for the CHARA Array. As before, we assume a physical size of 10 light days and $H_0 = 75\,km\,s^{-1}\,Mpc^{-1}$. Here the baseline is 1000 m.

As seen in Table 4, a much larger sample is accessible here. Two objects, NGC 4051 and NGC 4151, have expected angular sizes which might allow their surface structure to be investigated. There are many circumstances which might make even more objects accessible, some of which are based on initial assumptions. If the true value of H_o were as high as $100\,km\,s^{-1}\,Mpc^{-1}$, a total of five objects could have morphological analysis performed on them. The same result could be accomplished if the size of the BLR were 15 light days (which is the quantity with the largest potential for change). Pushing the envelope on the baseline is probably the only parameter which can be directly altered by the observer, but the same five objects can be reached if the baseline were 1500 m. Obviously, all of these quantities are interrelated. For example, if all three of the above conditions were met, a total of of ten objects can be analyzed in this manner.

There is clearly a great potential for exploration of the central engines of AGNs with optical

TABLE 4. Number of BLRs resolvable with a 1000 m baseline space-based interferometer in both Hα and Hβ given the parameters from Table 1, a physical size of 10 light days and $H_0 = 75\,\mathrm{km\,s^{-1}\,Mpc^{-1}}$. The resolution limits for 'limb darkening', the first correlation null and several values of the precision of correlation measurement are shown, assuming a required precision of 10% on the diameter measurement.

	No. of Objects Hα $\lambda = 656.3$ nm	No. of Objects Hβ $\lambda = 486.1$ nm
Limb Darkening	0	1
First Null	1	2
10%	6	10
2%	16	23
1%	23	32

interferometry. It will be possible to harvest the same sort of gains in the BLR with optical interferometry as were made on the structure of jets with radio interferometry. A fertile ground lies ready for the exploration of these beastly cosmic blow-torches.

6. REFERENCES

R. Antonucci, 1993, ARA&A, 31, 473.
T.A. ten Brummelaar, 1993, CHARA Array Final Report to NSF, Appendix R
T.A. ten Brummelaar, 1995, MNRAS, Submitted
T.A. ten Brummelaar, W.G. Bagnuolo & S.T. Ridgway, 1995, Opt. Let., 20, 521
D. Buscher, 1988, MNRAS, 235, 1203
J. Davis, 1981, *IAU Colloquium No. 62, Current Techniques in Double and Multiple Star Research, Lowell Observatory Bulletin No. 167*, eds: R.A. Harrington & O.G. Franz, (Lowell Observatory: Flagstaff), 191.
A.A. Michelson & F.G. Pease, 1921, ApJ, 53, 249.
H. Netzer, 1991, *Variability of Active Galaxies*, eds: W.J. Duschl, S.J. Wagner, & M. Camenzind, (Springer-Berlag: Berlin), 107.
S.T. Ridgway, 1994, CHARA Technical Report 2
W.J. Tango & R.Q. Twiss, 1980, Progress in Optics, XVII, 239
B.M. Peterson, 1993, PASP, 105, 247.
D.W. Weedman, 1977, ARA&A, 15, 69.